BRNO UNIVERSITY OF TECHNOLOGY
Faculty of Electrical Engineering and Communication
Department of Power Electrical and Electronic Engineering

Ing. Mustafa Osman Elrayah Aboelhassan

FAULT-TOLERANT CONTROL OF A FLUX-SWITCHING PERMANENT MAGNET SYNCHRONOUS MACHINE

ROBUSTNÍ ŘÍZENÍ SYNCHRONNÍHO STROJE S PERMANENTNÍMI MAGNETY A SPÍNANÝM TOKEM

SHORT VERSION OF **PH.D. THESIS**

Study Field: Power Electrical and Electronic Engineering
Supervisor: Prof. Ing. Jiří Skalický, CSc
Opponent:

Date of defense:

Keywords

Aerospace, High speed, Redundancy, Fault-Tolerant, AC motor drives, Fault-Tolerant machines, Dual three-phase machines, Flux-Switching permanent magnet synchronous machine (FS-PMSM), Multi-phase motors, Multi-phase drives, Vector-control, Field-oriented vector-control, Pulse-width modulation (PWM), Voltage source inverter (VSI), Permanent magnet synchronous machine (PMSM), Nonlinear-control, Feedback-control, Speed control, Current control, Field-weakening control, Normal-operating condition (Healthy), Faulty-operating condition (Unhealthy), Open-circuit fault, Short-circuit fault, Single-phase fault, Balance three-phase fault, Braking-torque, Safety-critical application.

Klíčová slova

Letecký, Vysokorychlostní, Nadbytek, Odolné proti poruchám, Frekvenční měniče, Odolnost vůči poruchám stroje, Dvojité trojfázové stroje, Pulzní tok permanentní magnety synchronního stroje, Vícefázové motory, Vícefázové pohony, Vektorové řízení, Polem orientované vektorové řízení, Pulsní šířková modulace, Napěťový měnič, Synchronní stroj s permanentními magnety, Nelineární řízení, Řízení zpětnou vazbou, Řízení rychlosti, Proudová regulace, Regulace odbuzováním, Normální provozní podmínky, Chybový provozní stav, Porucha naprázdno, Porucha zkratem, Jednofázové poruchy, Nerovnováha tří fází, Brzdný moment, Bezpečnostně kritické aplikace.

Místo uložení práce

Práce je k dispozici na Vědeckém oddělení děkanátu FEKT VUT v Brně,
Technická 3058/10,
Brno, 616 00

CONTENTS

1. INTRODUCTION

FLUX-SWITCHING machines are gaining an increasing popularity in high-performance drives due to their numerous advantages over other brushless machines [1], [2]. Their rotor structure is similar to that of a switched reluctance machine with all the associated advantages in terms of robustness and construction simplicity. They are, however, an ac machine having a sinusoidally varying permanent-magnet (PM) flux linking each phase winding with rotor rotation. They can thus be sinusoidally driven and have the associated advantages of sinusoidally excited machines including a smooth output torque and constant input power in steady-state balanced operation. The output torque can be dynamically controlled using vector-control algorithms. In this paper, a control scheme for a fault-tolerant-flux-switching-machine design will be presented. The machine itself was designed to have two sets of three-phase windings, each supplied from a separate three-phase converter drive. The drive-system behavior in healthy-conditions and when it undergoes a variety of faults will be looked at, and results from an experimental drive system will be detailed.

Fault-tolerance is often adopted in safety-critical drive systems such as aerospace drives to reach the required drivesystem reliability levels with minimum overall weight and component count. The fundamental concept is to have redundancy in the components which are more likely to fail rather than have redundancy at the drive-system level. This usually requires isolation (thermally, electrically, magnetically, and physically) from each component to avoid failure propagation [3]. Electrical machines can be made to be fault-tolerant in different configurations depending on the nature of faults they need to tolerate. The failures which are more likely to occur in an electrical drive system are those related to the converter drive including sensors; active and passive components; and related driving, control, and protection circuitry. Within the machine itself, the main failure modes which need accounting for are winding and bearing failures. Bearing failures are progressive and diagnostic, and prognostic techniques can be employed to cater for these. With electrical failures in the converter and machine, remedial action needs to be taken to ensure drive operation in safety-critical applications.

Different machine topologies have been proposed for such applications. PM machines have often been chosen based on their higher specific torque and power density [4]. Concentrated wound machines designed to have a high phase inductance and low phase–phase mutual inductance and fed from separate converters were shown to fulfill these fault-tolerant requirements. The main challenge with the design of such machines is the magnet permanent field excitation which cannot be disabled in case of a fault unless some type of complex mechanical mechanism or active magnet shunts are used as reviewed in [5]. These are often not acceptable due to increased complexity and weight and due to their implication on the system reliability. The requirement for high inductance to limit the short-circuit current results in a low machine power factor, and if the machine is used in a variable speed application, the braking-torque generated when the machine is running at low speeds can be significant.

Flux-switching machines can be seen as very similar, in terms of machine terminal behavior, to PM machines as described earlier on. Having their magnets embedded in the stator will reduce the copper area available for the winding; however, as the magnets are in a fluxfocusing arrangement, a relatively good torque density can be achieved. Fault-tolerant PM machines are also often limited by the maximum magnet temperature limit. As is well known [6], concentrated fractional pitch machines display a harmonic-rich armature field which can induce substantial losses in the magnets themselves and any other rotor conducting components, particularly retaining cans. Although rotor losses are typically much lower than the stator losses, their thermal path has a much higher thermal resistance to the cooling surface, thus limiting the maximum torque achieved. This problem is generally exacerbated when a fault occurs and a fault-tolerant control is applied [7]. Although the fundamental synchronous rotating armature field is generally restored when a fault-tolerant control strategy is applied, the harmonic content of the armature field, particularly the triplen harmonics, increases significantly the rotor losses.

The problem of rotor losses originating from the armature field in PM machines can be significant if cooling is only arranged through the stator housing. These losses can quickly translate in high magnet temperature due to the high-thermal-resistance air-gap. This limits the allowed armature reaction field and consequently torque. Flux-switching machines have an important advantage in such situations in that the magnets have a much improved thermal path to the machine housing, and rotor magnet retention is of course not needed, thus significantly reducing the overall losses and this constraint.

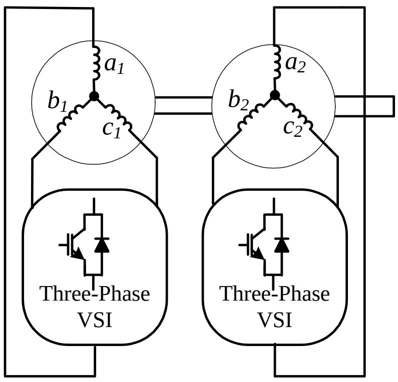

Figure 2.1.1 *Standard two-machine setup with machines in torque-summing configuration*

2. FAULT-TOLERANT DRIVE SYSTEMS

Drive-system reliability can be typically improved by increasing the number of machine-converter units, or the number of phases, or the number of winding channels or a combination of the aforementioned in order to ensure continued operation in case of a fault occurring. *Figure 2.1* and *Figure 2.2* show common ways how this modularity can be achieved. If separate-phase current control is adopted, *Figure 2.2 (a)*, a specific fault-tolerant control strategy to deal with open-circuit and short-circuit faults needs to be implemented. This usually relies on a fault-detection and location algorithm to reconfigure the control accordingly. In addition, this configuration suffers from additional torque and input current ripple [8]. This work is based on a dual three-phase channel machine similar to that in *Figure 2.2* (b). Each machine (three-phase channel) is fed from a separate three-phase converter. In case of a phase open-circuit fault in one of the machine-drive units, the postfault control strategy is to disable the faulty-unit and deliver power with the remaining healthy-unit. In case of a short-circuit fault, the post-fault control strategy is to apply a balanced short-circuit through the converter and again continue operation with the healthy-unit, this time having to additionally overcome the braking-torque produced by the faulty-unit. These types of control strategies have been implemented for both concentrated wound PM machines [9] and induction machines [10] showing their respective implications on drive operation. This work will present the modeling and implementation of a fault-tolerant vector-control strategy for flux-switching machines and will highlight the implications of adopting such a system.

2.1 FAULT-TOLERANT FLUX-SWITCHING MACHINE

Flux-switching machines have numerous inherent advantages for achieving high power density as discussed in the introductory section; however, in their basic form, they are not tolerant to short-circuit winding failures. In [11] and [12], a new design concept was introduced, which is able to make the machine fulfill the fault-tolerant requirements. In [13] and [14], a similar concept is adopted for a 12-slot–14-pole machine. Depending on the stator slot–rotor pole combination, flux-switching machines offer various possibilities to achieve a dual three-phase channel winding [15]. For the flux-switching machine under consideration, a channel split described in *Figure 2.3* is considered [12].

The most popular slot–pole combinations are 12 slots–10 poles and 12 slots–14 poles derived from the “minimal” combinations of six slots–five poles and six slots–seven poles, respectively [16]. In [17], it has been shown that the sixslot–seven-pole-based combination has a higher torque density than the more popular six-slot–five-pole configuration. Due to this and to use a reasonable electrical frequency at the relatively high speed of 7600 r/min, the machine opted for has seven rotor poles. This is equivalent to seven pole pairs for PM synchronous machines. In [18] and [19], the control of a 12-slot–10-pole flux-switching machine is considered.

The control adopted is based on hysteresis current controllers, and the authors have investigated the operation of the machine from a dual three-phase converter unit under open-circuit faults. This thesis will mainly look at a machine operation with short-circuit faults and fed by an SV-PMW control. In the event of a winding short-circuit fault due to device or winding failure, the fault current should be limited to a safe level to preserve the machine integrity. One per unit (*p.u.)* phase self-inductance is commonly adopted in order to limit the short-circuit current to the rated value [9], [20]. This based on the nominal voltage, rated power, and nominal operating frequency. As discussed, another requirement is that any faulty-part of the machine does not significantly influence the remaining healthy-part. Winding layouts such as single-layer technology can be used to meet these requirements [12]. In this paper, the machine adopted uses a semiclosed slot configuration with spacer teeth to achieve *1-p.u.* self-inductance as well as excellent magnetic and physical decoupling between any two nearby coils as shown in *Figure 2.3.*

The main aims of the spacer-tooth, as is in alternate concentrated-wound PM machines, are thus to minimize mutual inductance and to rule out the possibility of phase–phase faults within the machine as well as to limit failure propagation through thermal means. The spacer-teeth thickness and the slot opening geometry are sized to meet the fault-tolerant requirements of minimal mutual-phase coupling and unity p.u. self-inductance as described in [12]. The spacer-teeth thickness is used as a design variable to reduce the mutual inductance. This, however, does not have a significant effect on the self-inductance. Sizing the slot opening is an effective way to set the phase inductance to *1 p.u.* [20].

When compared to a machine of the same size but not designed to be fault-tolerant, the machine earlier produces a lower torque and has a lower power factor due to the higher leakage paths. This is the same as for PM synchronous machines.

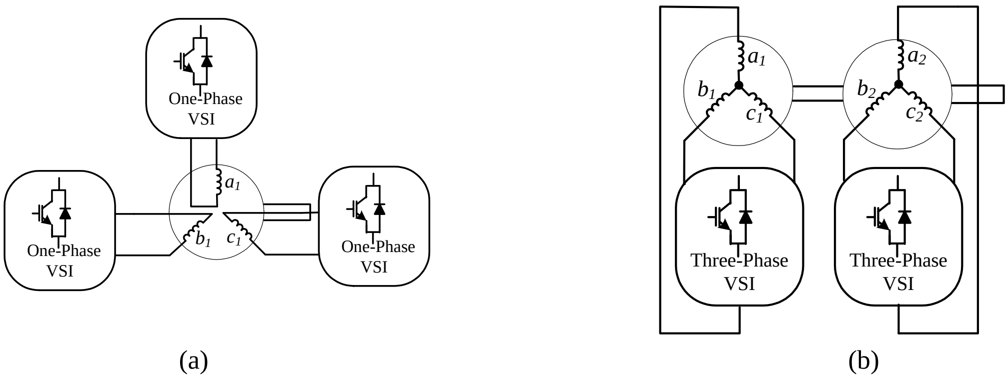

Figure 2.2 *Electrical redundancy (power supply and converters) can be achieved either through (a) separate phase current control or through (b) dual three-phase channel machine*

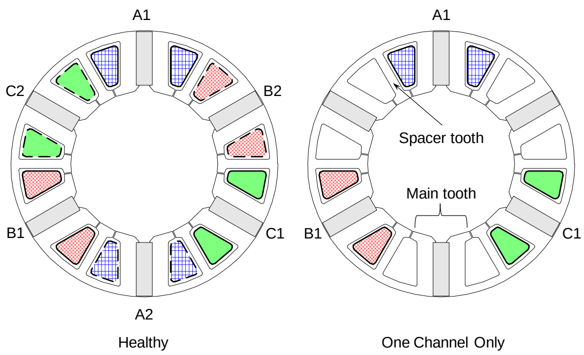

Figure 2.3 *Channel split configuration of the dual-channel FS-PMS*

2.2 FLUX-SWITCHING-MACHINE MODEL

A machine model based on a phase equivalent circuit was adopted to enable drive simulation in both healthy- and faulty-conditions. A mathematical (*a1, b1, c1*) and (*a2, b2, c2*) model of the dual three-phase flux-switching PM synchronous machine (FS-PMSM) will be briefly described in this section. This can be derived in the same way as for a PM synchronous motor. The phase voltages supplied to the stator windings (v_{a1}, v_{b1}, v_{c1}) of the first three-phase star-connected winding set are defined as

$$v_{a1} = r_s i_{a1} + \frac{d\psi_{a1}}{dt} \tag{2.1}$$

$$v_{b1} = r_s i_{b1} + \frac{d\psi_{b1}}{dt} \tag{2.2}$$

$$v_{c1} = r_s i_{c1} + \frac{d\psi_{c1}}{dt} \tag{2.3}$$

where i_{a1}, i_{b1}, and i_{c1} are the phase currents in the stator windings; *rs* is the phase resistance; while ψ_{a1}, ψ_{b1}, and ψ_{c1} are the stator flux linkages of the first motor unit. Similarly, for the second winding set (a_2, b_2, c_2), the equations earlier can be rewritten with a subscript of two instead of one.

The stator flux linkage can be expressed as

$$\psi_{a1} = \left(L_{ls} + \bar{L}_m\right) i_{a1} - \frac{1}{2}\bar{L}_m i_{b1} - \frac{1}{2}\bar{L}_m i_{c1} + \psi_m \sin\theta_r \tag{2.4}$$

where L_{ls} and L_m are the stator magnetizing- and leakage-inductances, respectively, while ψ_m is the magnitude of the flux linkages established by the PM. This assumes no coupling between the two-machine units. Although there is some mutual coupling between the two-machines as shown in *Figure 2.4*, this has been ignored as its mean value is relatively small compared to the coil self- inductance.

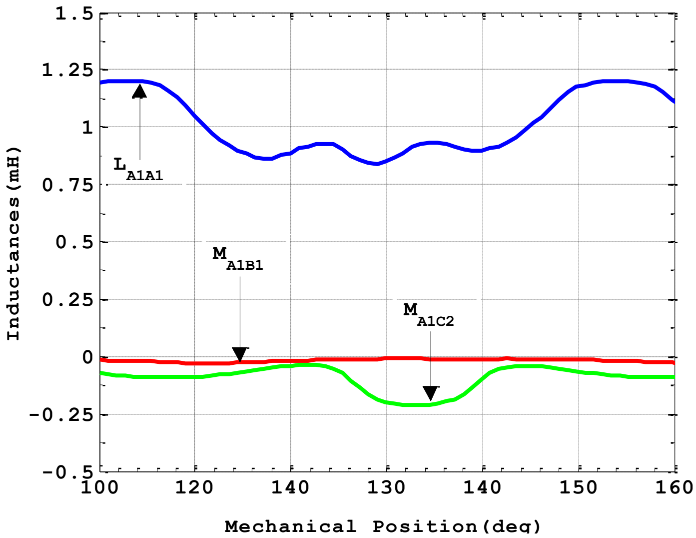

Figure 2.4 *Self-inductances and mutual-inductances for fault-tolerant FS-PMSM*

The coupling reduces further as the machine is loaded. A $d-q$ representation of the machine can be adopted due to the sinusoidal nature of the phase flux-linkage variation with rotor position. As in conventional PM machines, the d-axis is taken to be aligned with the magnet flux linkage. Correspondingly, the induced B-EMF is aligned to the quadrature axis. The electromagnetic torque is composed of two-parts. The first part is the PM torque which arises from the interaction of the magnet flux and q-axis stator current component. The second part is the reluctance-torque component caused by the inductance variation as a function of the rotor position.

Figure 2.5 shows the *d* and *q* inductances as a function of position. The saliency is minimal and goes virtually to zero with load. Therefore, the reluctance-torque is negligible, and the control strategy adopted is similar to that of a nonsalient PM synchronous machine [21]. Due to the nature of the machine, the machine parameters vary significantly with load and position. In order to have a realistic representation of the machine, finite-element analysis was used to determine the PM flux linkage as a function of position and load and the self-inductances and mutual-inductances as a function of position and load.

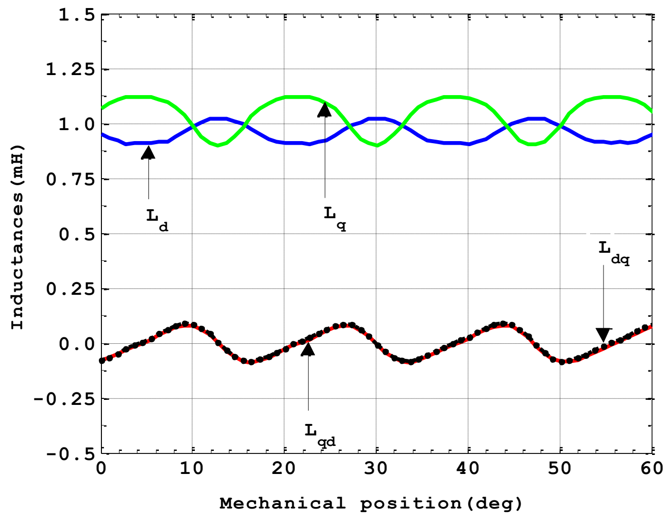

Figure 2.5 *Direct- and quadrature-inductances for fault-tolerant FS-PMSM*

These were integrated within the model as lookup tables. *Figure 2.4* shows the machine inductance as a function of position at no load.

The electromagnetic-torque equation of one motor unit (e.g., a_1, b_1, and c_1) can be then evaluated as in the following:

$$T_{e1} = \frac{P\psi_m}{2}\left(i_{a1}\cos\theta_r + i_{b1}\cos\left(\theta_r - \frac{2}{3}\pi\right) + i_{c1}\cos\left(\theta_r + \frac{2}{3}\pi\right)\right) \tag{2.5}$$

Therefore, the total electromagnetic-torque of the dual three-phase flux-switching PM motor can be obtained from the torque of both motors, as shown in the following:

$$T_{e-total} = (T_{e1} + T_{e2}) \tag{2.6}$$

The drive's mechanical characteristics can be expressed as in

$$\frac{d\omega_r}{dt} = \left[\frac{P}{(2J)}(T_{e-total})\right] - \frac{B_m}{J}\omega_r - \frac{P}{2J}T_L \tag{2.7}$$

where P is the number of electrical poles (i.e., twice the number of rotor poles), T_L is the load-torque applied, B_m is the viscous friction coefficient, and J is the equivalent moment of inertia of the drive system.

The electrical angular velocity is the derivation of the displacement electrical angle and can be described by

$$\frac{d\theta_r}{dt} = \omega_r \tag{2.8}$$

where, ω_r and θ_r are the electrical angular velocity and displacement of the adopted reference frame, respectively.

3. SIMULATION RESULTS

The model described earlier can be easily programmed into most simulation environments and has a fast solution time. For the work undertaken here, the model was incorporated into a *Matlab/Simulink* model of the full motor-drive system, including a vector-control algorithm orientated with the PM flux linkage and a mechanical load model. The inverter in this case has been modeled by ideally controlled voltage sources but could easily be extended to incorporate real device models if required. *Figure 3.1* shows the d and q current components during a speed transient, followed by the application of a $1\text{-}N \cdot$ m load step at $t = 7.5$ s and an open-circuit fault at $t = 10$ s, respectively. The drive system is speed controlled. As expected, the variation of i_{q1} and i_{q2} is proportional to the torque produced by the respective machine unit. It can be observed that the torque is equally shared by the machine units until the open-circuit fault. At $t = 10$ s, when an open-phase condition is introduced to motor 2, motor 1 picks up the entire load.

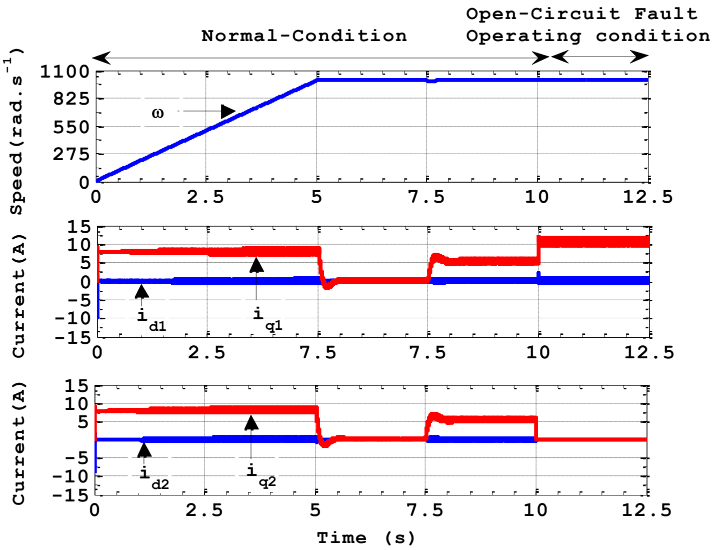

Figure 3.1 *Behavior of the FS-PMSM at the speed of 1000 rad/s under normal- and open-circuit fault operating conditions*

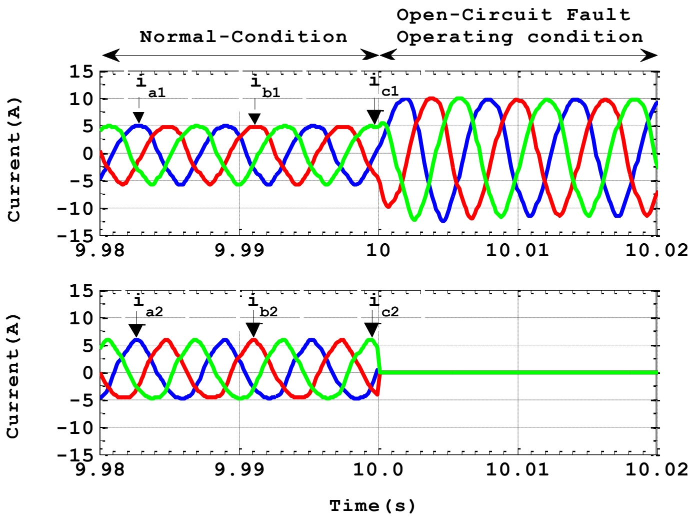

Figure 3.2 *Currents behavior of the FS-PMSM at the speed of 1000 rad/s under normal- and open-circuit fault operating conditions.*

Figure 3.2 shows the two motors' phase currents before and after the fault occurs. It can be observed that the simulated phase currents of the two-machine units (*Figure 3.2*) contain a significant amount of even harmonics, which is in the nature of this machine topology as will be further demonstrated later on in the experimental tests.

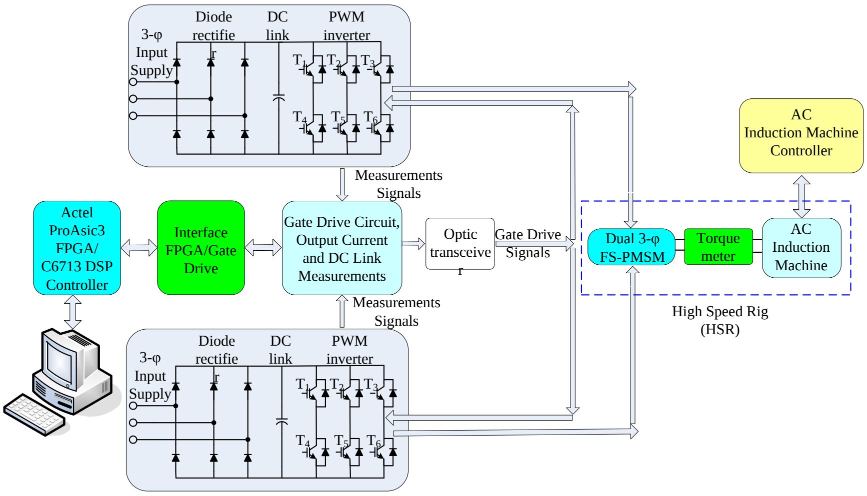

Figure 3.3 *Block diagram of the experimental system*

4. EXPERIMENTAL DRIVE SYSTEM

A vector-controlled dual three-phase inverter and machine were set up on an instrumented test rig as shown in *Figure 3.3* and *Figure 3.4*. The machine coils were separately brought out to enable us to experiment with different winding connections and apply faults to different winding locations. The machine was loaded using a vector-controlled induction machine with a rated power of *60 kW* at *20 000 r/min* coupled through a torque transducer as shown in *Figure 3.4*.

The overall vector-control scheme adopted is shown in *Figure 3.5* where the torque demanded by the speed loop is shared equally by the two-motor units in healthy-operation. The field-orientated scheme is implemented on a control board consisting of a Texas Instruments *C6713 processor* and *Actel ProAsic3 FPGA*. The PWM switching signals are transmitted to the gate drivers using high-performance fiber-optic links.

The two three-phase channels of the FS-PMSM are fed from separate converter units as shown in *Figure 2.2* (b) and *Figure 3.4*. The rotor position is obtained from a resolver transducer. The six stator- pole seven-rotor-pole flux-switching machine was constructed from *0.35*-mm silicone steel laminations and samarium cobalt PMs. The machine was totally enclosed and naturally ventilated.

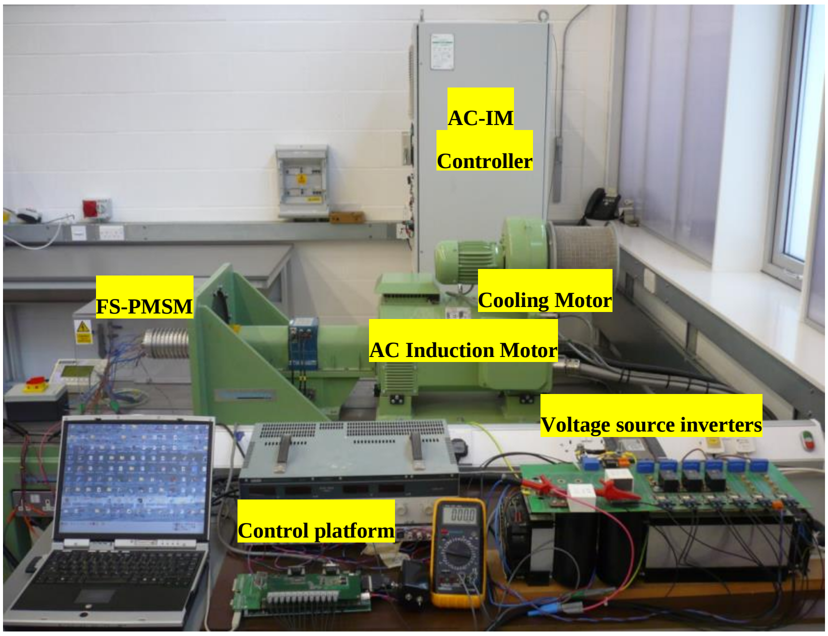

Figure 3.4 *Experimental setup*

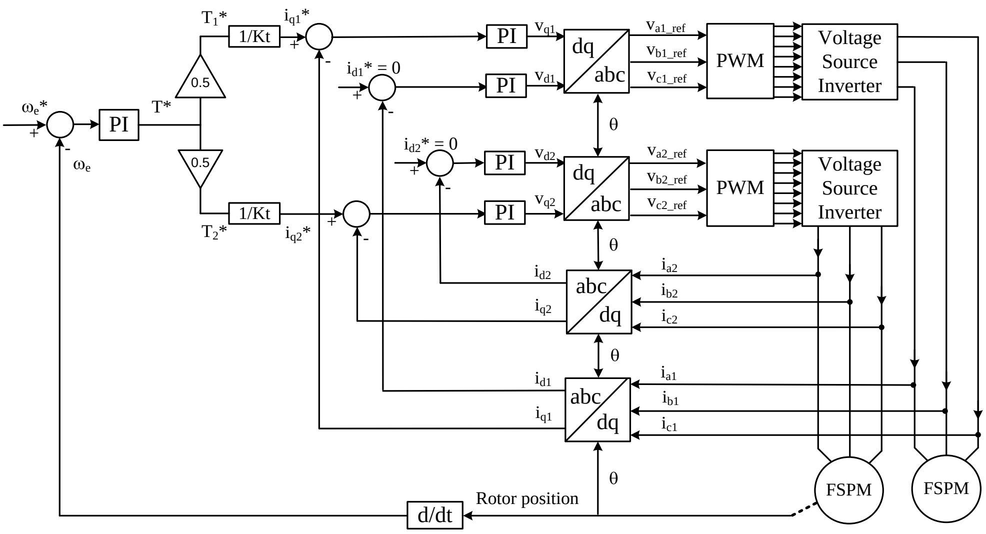

Figure 3.5 *Vector-control structure of dual three-phase flux-switching PM motor under-normal operating condition.*

Figure 3.6 shows the no-load B-EMF of the different stator coils. It can be noted that the waveform is distorted with even harmonics. It can also be observed that the respective phase B-EMFs of each machine module have the even harmonics in phase opposition with respect to each other. These would naturally cancel each other out if the dual-channel machine was to be connected as a single three-phase machine with the phase coils connected in series.

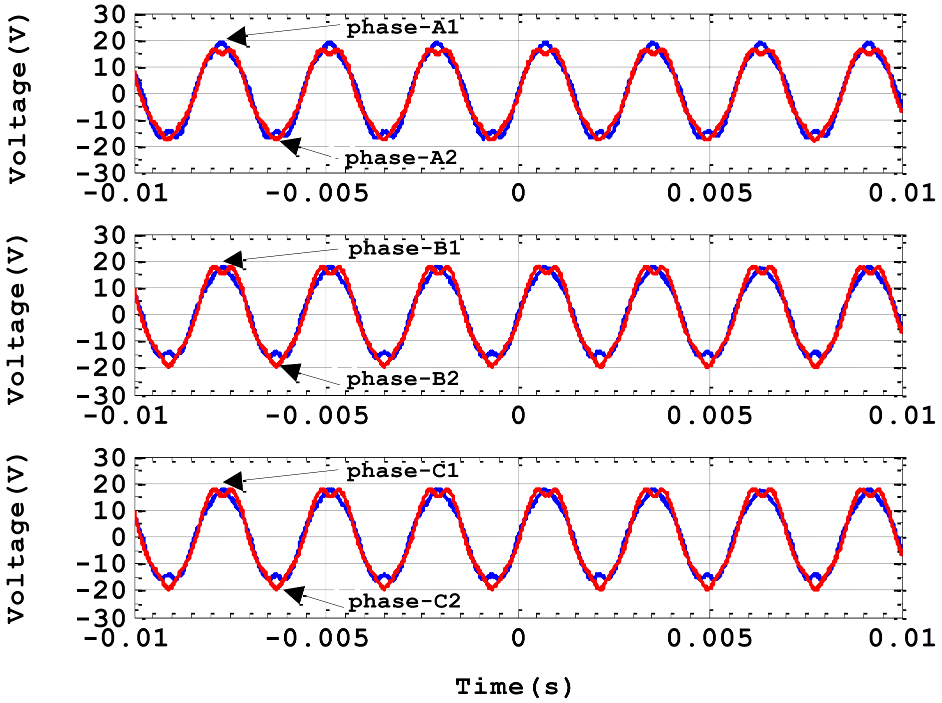

Figure 3.6 *B-EMF plots of the dual-channel three-phase machine.*

4.1 STEADY-STATE PERFORMANCE

The first tests were performed to verify the steady-state performance of the machine units. *Figure 3.7* shows the measured torque as a function of q-axis current at a speed of *500 r/min*.

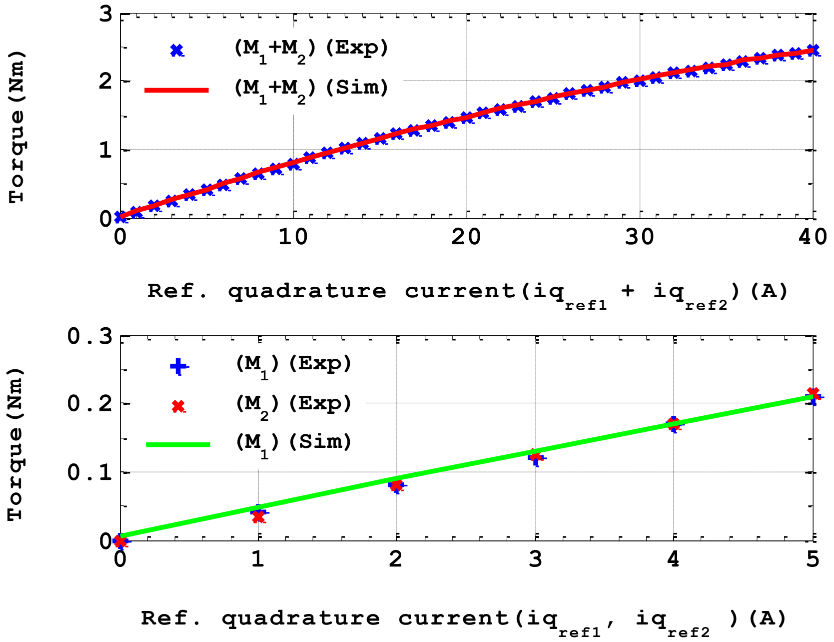

Figure 3.7 *Torque of dual three-phase FS-PMSM: (a) Normal-condition and (b) open-circuit condition.*

It can be observed that the two-machine units produce similar torque values. The torque values shown are those measured minus the torque measured without any excitation (no-load loss). This was done in order to have a direct comparison with the simulated results. It can be observed from *Figure 3.7 (a)* that, beyond $i_{q1} + i_{q2} = 10\ A$, the two-machine units display a reducing torque constant due to magnetic saturation.

Figure 3.8 shows the total measured and simulated braking-torque as a function of speed when both machines are short-circuited in a balanced way. In this case, the machines are driven by the induction motor on the experimental rig. It can be observed that the model developed offers a close representation to the real machine behavior. As expected, the results show a reducing braking-torque as speed increases and as the inductive reactance becomes more dominant.

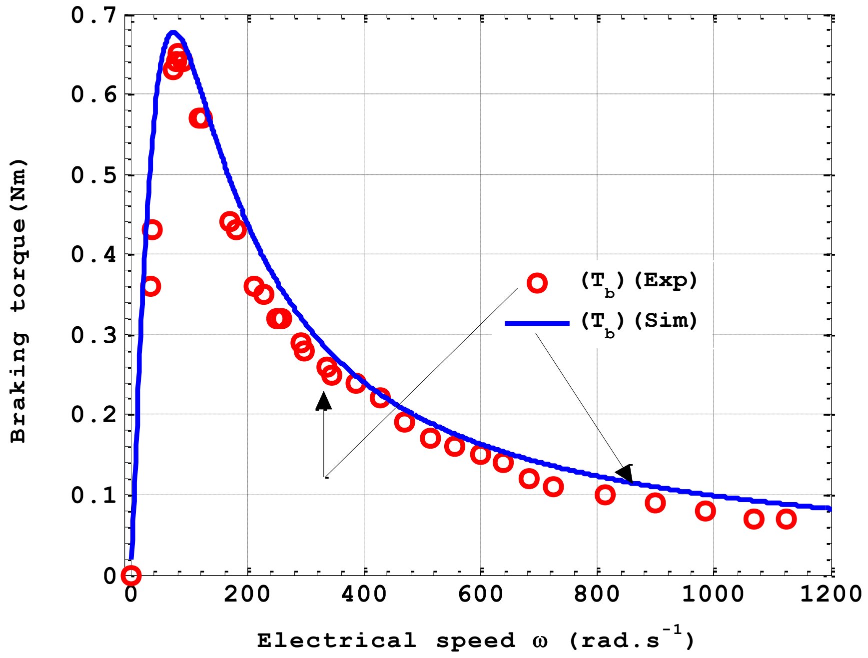

Figure 3.8 *Braking-torque of dual three-phase FS-PMSM with the peak braking-torque appearing at 82 rad/s.*

The experimental tests were carried out by feeding the dual-channel FS-PMSM via two-independent vector-controlled voltage source inverters. *Figure 3.9* shows the experimentally measured steady-state short-circuit current (i_{sc}) values of the faulty-motor during a balanced three-phase short-circuit operating condition at different speeds. In this case, the fluxs-witching machine drive system was operated in speed-control with the induction machine providing a loading-torque. With one flux-switching-machine unit short-circuited, the healthy-machine unit had to overcome the loss of torque of the faulty-machine plus additional torque to overcome the braking-torque. The plot also illustrates the *q-axis* current component of the remaining healthy-machine which varies as a function of speed in order to compensate for the speed-dependent braking-torque generated by the shorted-machine. It is worth noting that, when a machine unit experiences a short-circuit fault, as explained earlier, the remaining unit takes over to deliver the remaining torque by doubling the *q-axis* current component to a linear approximation as well as needing an additional overhead to mitigate the braking-torque. This will result in a much higher machine thermal loading as the faulty-unit would produce losses proportional to the fault current squared, and the healthy-unit will see its losses increase proportionally to the square of the *q-axis* current.

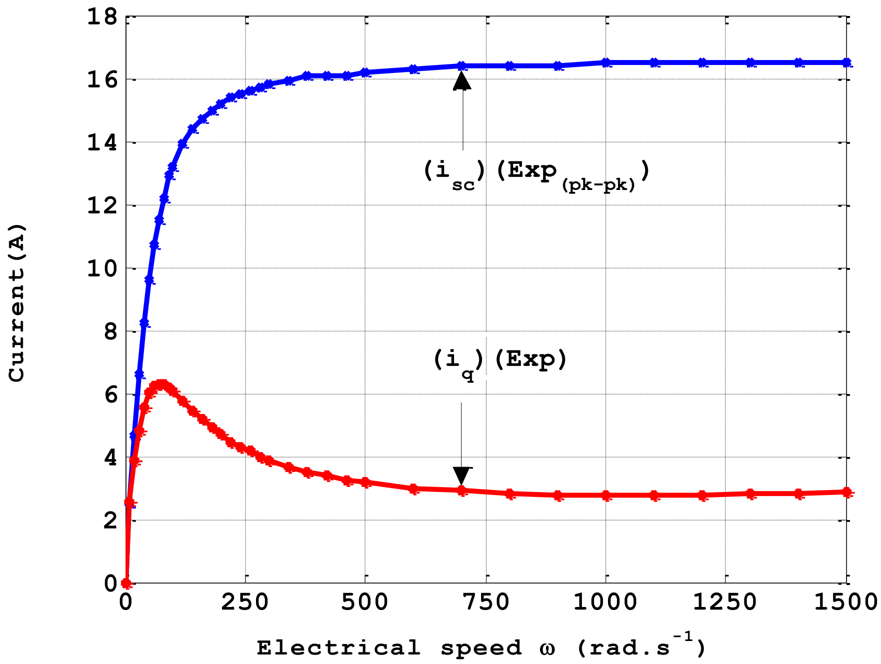

Figure 3.9 *Dual three-phase FS-PMSM: One-phase short-circuit (pk-pk) current and quadrature current of the remaining motor as the function of speed.*

4.2 TRANSIENT PERFORMANCE

This section will present the transient behavior of the dual-channel flux-switching machine during both healthy- and faulty-conditions. The robustness of the drive operating during open- and short-circuit converter faults will be demonstrated in this section.

When a winding short-circuit is detected, the machine terminals are shorted to limit the fault current to a value below rated, and the remaining three-phase winding set is used to produce the torque requirement. *Figure 3.10* shows the phase currents of the dual three-phase motors before and after an open-circuit fault occurs at *1000 r/min*. It can be seen that the resulting output torque is maintained as a result of doubling the healthy-machine current. When a balanced three-phase short-circuit is present in a one-machine unit, a speed-dependent braking-torque will be produced. A balanced three-phase fault is applied after any converter or motor short-circuit failure. In order to attain a good dynamic performance, the braking-torque is estimated from the fault current of the faulty-machine unit and compensated for in a feed-forward fashion to the healthy-motor unit. The implemented system is shown in *Figure 3.11*. In the presence of a short-circuit fault, the proposed torque compensation scheme is applied to the healthy-channel of the FS-PMSM after a balanced short-circuit is applied across the faulty-machine channel. This requires a diagnostic methodology able to detect the fault-occurrence. As it can be observed, assuming motor unit M_1 is shorted, the *q-component* of the short-circuit current is used in the feed-forward compensation. This current component is speed dependent, and two inaccurate assumptions are made. The first is that there is no saliency torque in the machine, i.e., the *d-component* of the short-circuit current is not producing any torque. The second is that the torque constant is assumed constant.

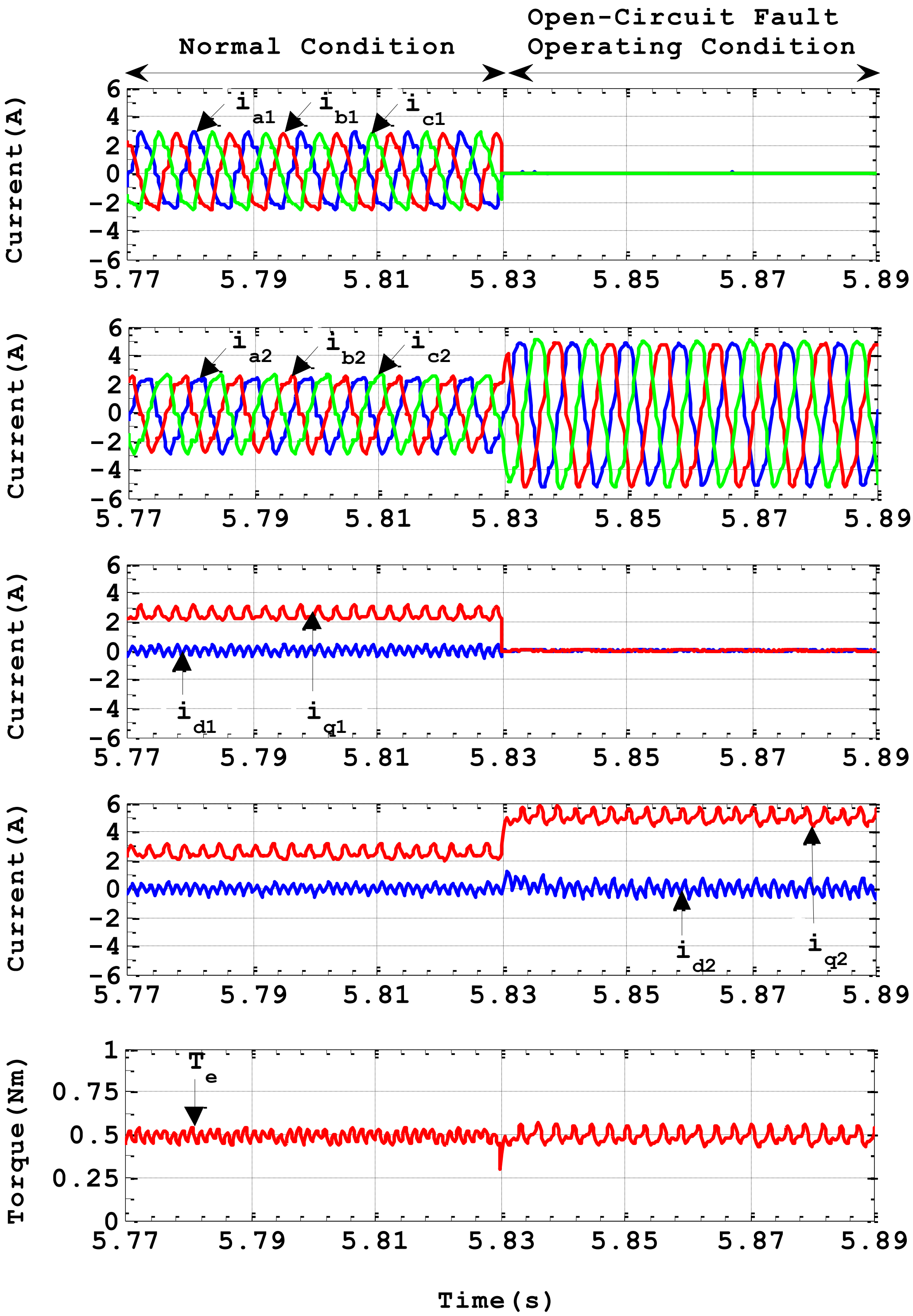

Figure 3.10 *Experimental performance of the proposed dual FS-PMSM (M_1 is open-circuited) under normal-mode of operation and three-phase open circuit. (a) Currents of motor 1. (b) Currents of motor 2. (c) Transformed currents of motor 1. (d) Transformed currents of motor 2. (e) Total motor-torque.*

Both assumptions are inaccurate as there is a small saliency, and the *d-component* of the short-circuit current will alter the magnetic circuit saturation level which will in turn affect the torque constant. In spite of these inaccuracies, adding the compensation strategy significantly improves the machine's dynamic performance.

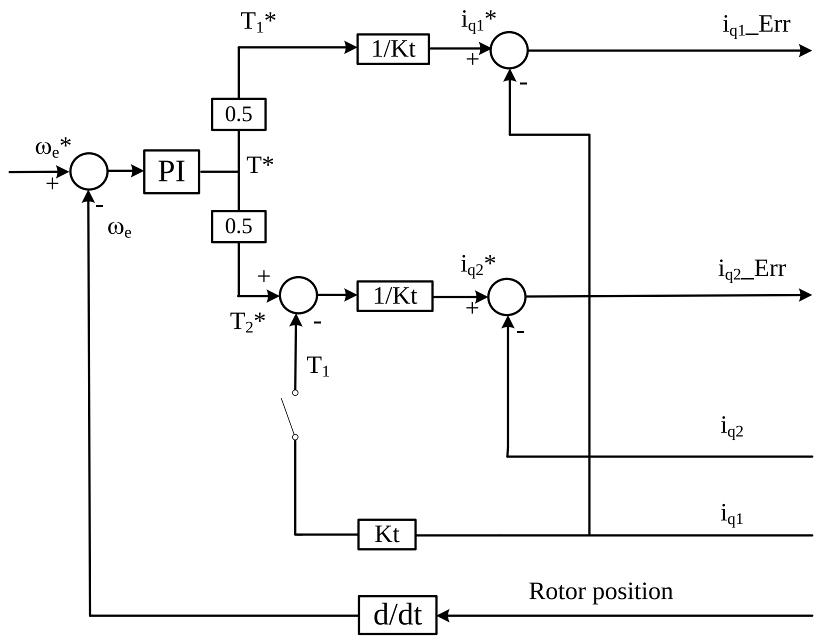

Figure 3.11 *Experimental Torque-compensation when motor 1 is short-circuited*

Figure 3.12 shows the two-machine-unit phase currents before and after a balanced short-circuit fault is applied on motor 1.

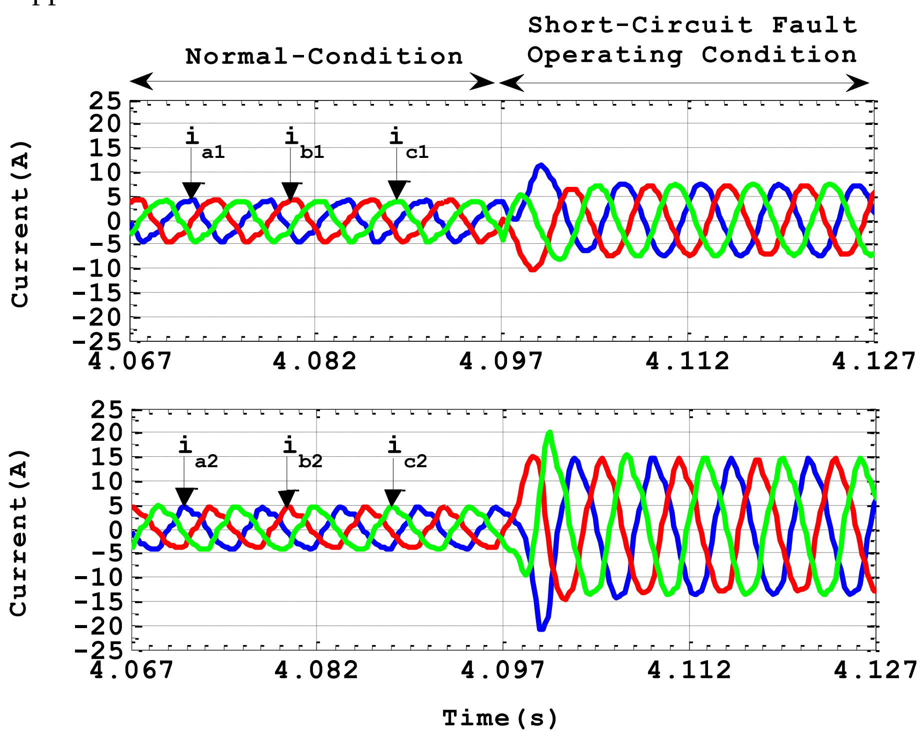

Figure 3.12 *Experimental performance of the proposed dual FS-PMSM (M_1 is short-circuited) under-different operating conditions. (a) Currents of motor 1.* (b) Currents of motor 2.

Figure 3.13 shows the corresponding drive behavior. It can be observed that the speed is maintained with motor 2 having to overcome the lost torque from motor 1 as well as the braking-torque due to the short-circuit currents. In this case, i_{q1} is fed-back to compensate for the braking-torque. This resulted in the current increasing by *160%* in the healthy-machine and by *40%* in the faulty-one. Naturally, this increase is speed and load dependent according to the braking characteristic shown in *Figure 3.8.*

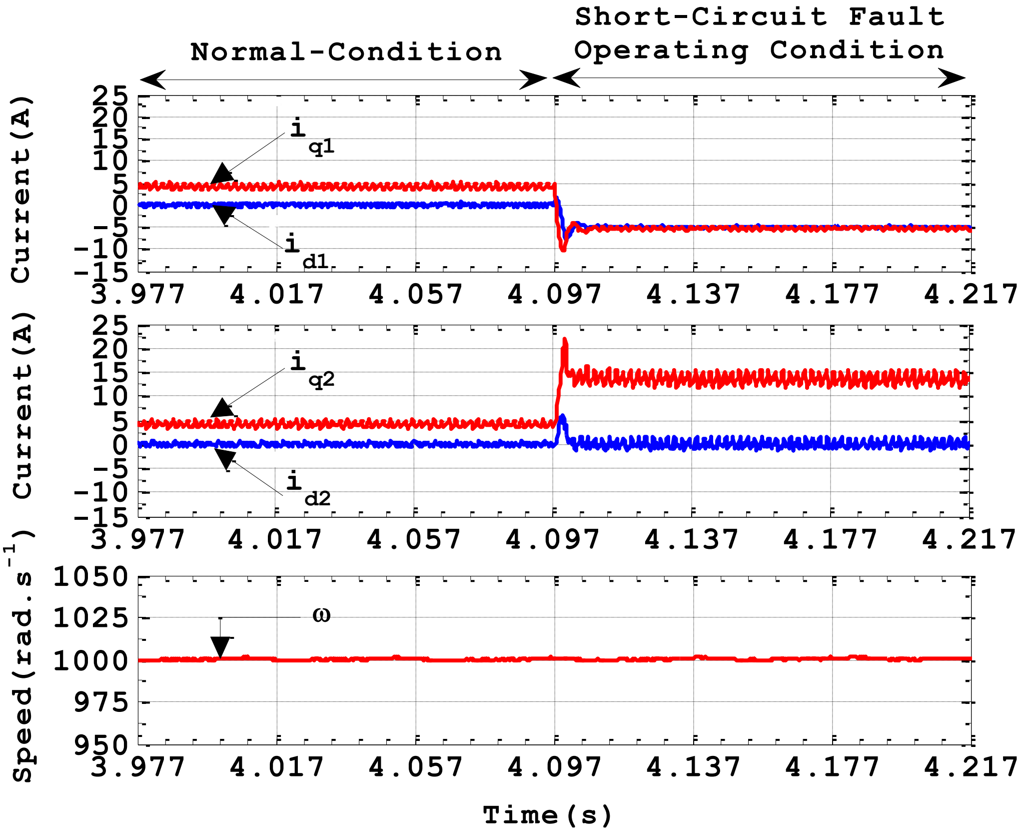

Figure 3.13 *Experimental performance of the proposed dual FS-PMSM (M_1 is short-circuited) under normal-mode of operation and under a balanced shor-tcircuit condition. (a) Transformed currents of motor 1. (b) Transformed currents of motor 2. (c) Motor speed.*

Figure 3.14 shows the experimental setup to test this condition. As is demonstrated in this figure, phase A of motor 2 can be shorted through an external contactor. This exact fault condition is not likely to occur in a practical scenario; however, it is representative of an internal winding failure. The most likely electrical failure is within the converter [8], and this condition has been evaluated in the preceding experiments. In safety-critical applications, it is however sometimes necessary to consider the drive performance when an internal motor fault occurs. In the machine structure considered, only faults within the same coil are possible due to their physical isolation. As a worst case scenario in terms of torque disturbance in a random wound coil, an entire coil short-circuit is considered.

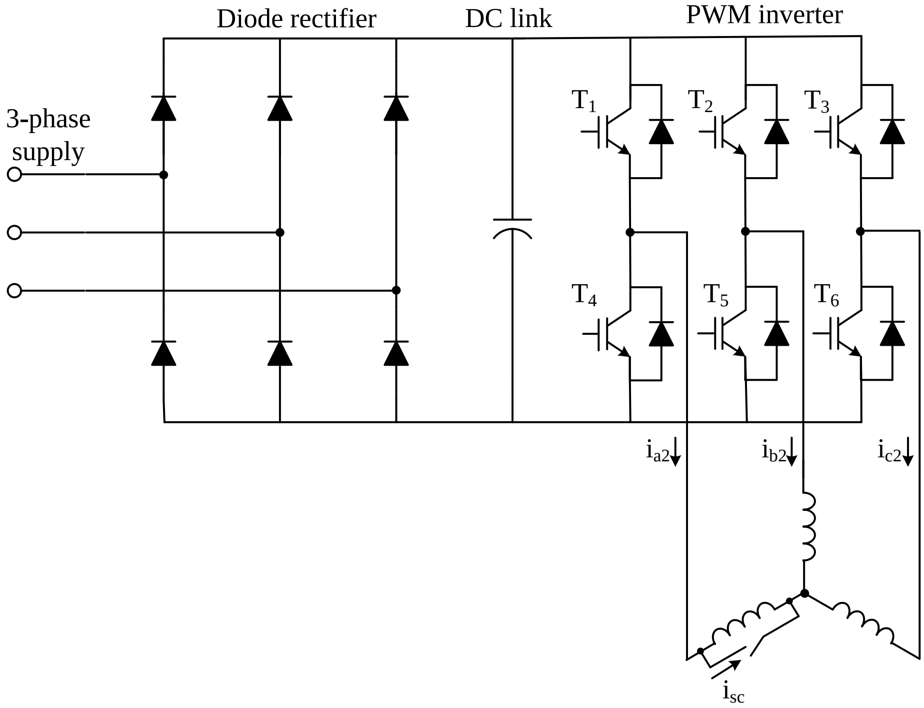

Figure 3.14 *FS-PMSM under short-circuit fault conditions.*

The motor is initially operated under normal-condition, and then, a single-phase fault is introduced. After a period of time, a balanced three-phase short-circuit fault (simultaneous short-circuit across all the three-phases) is applied to the faulty-motor through the converter. The measured currents are plotted in Figs. 3.15 – *3.17*.

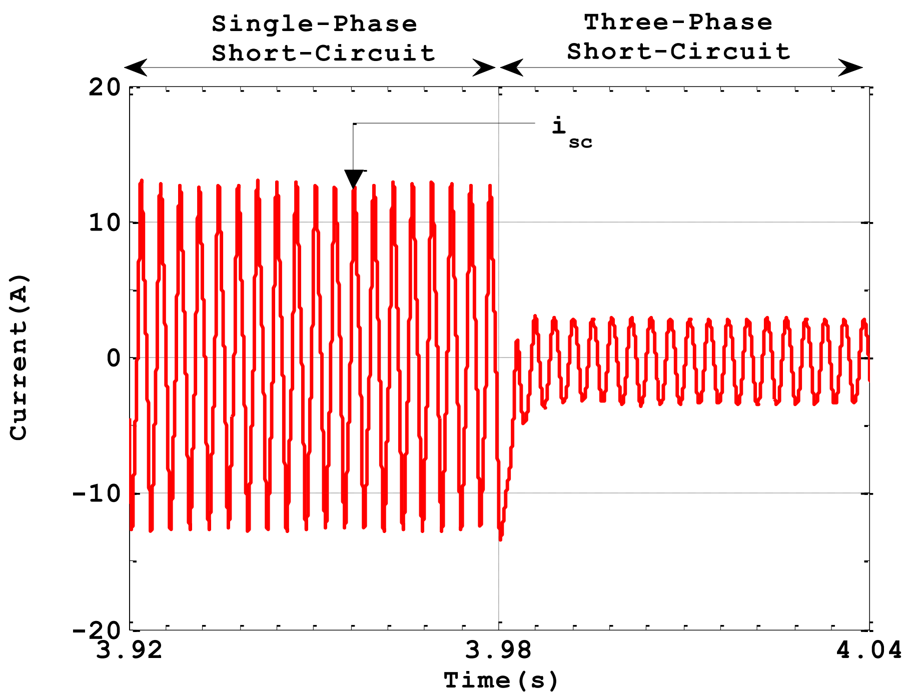

Figure 3.15 *Experimental short-circuit current under different- operating conditions (M_2 is short circuited) at the speed of 2000 rad/s.*

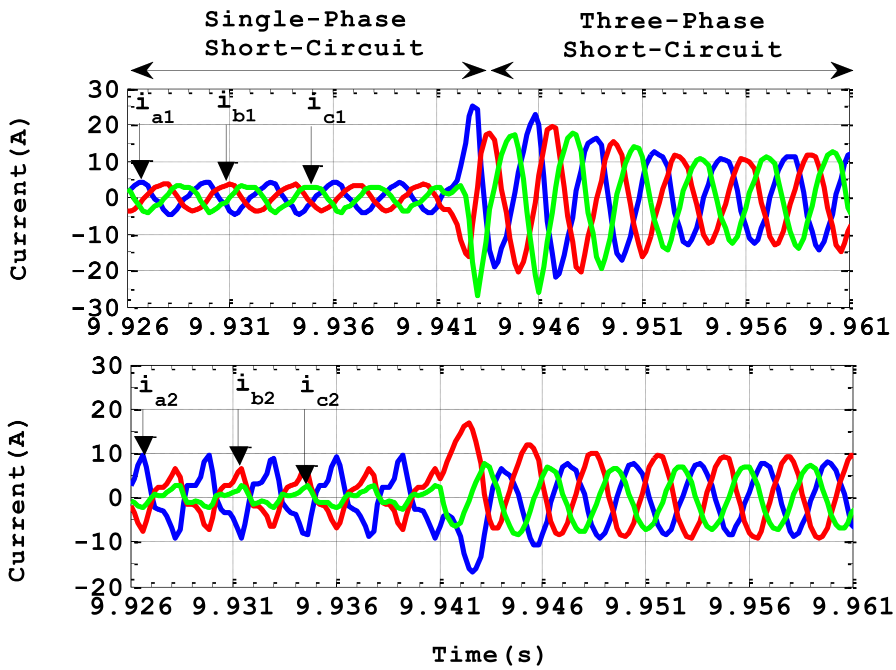

Figure 3.16 *Experimental performance of the proposed dual FS-PMSM (M_2 is short-circuited) under single- and balanced short-circuit conditions. (a) Currents of motor 1. (b) Currents of motor 2.*

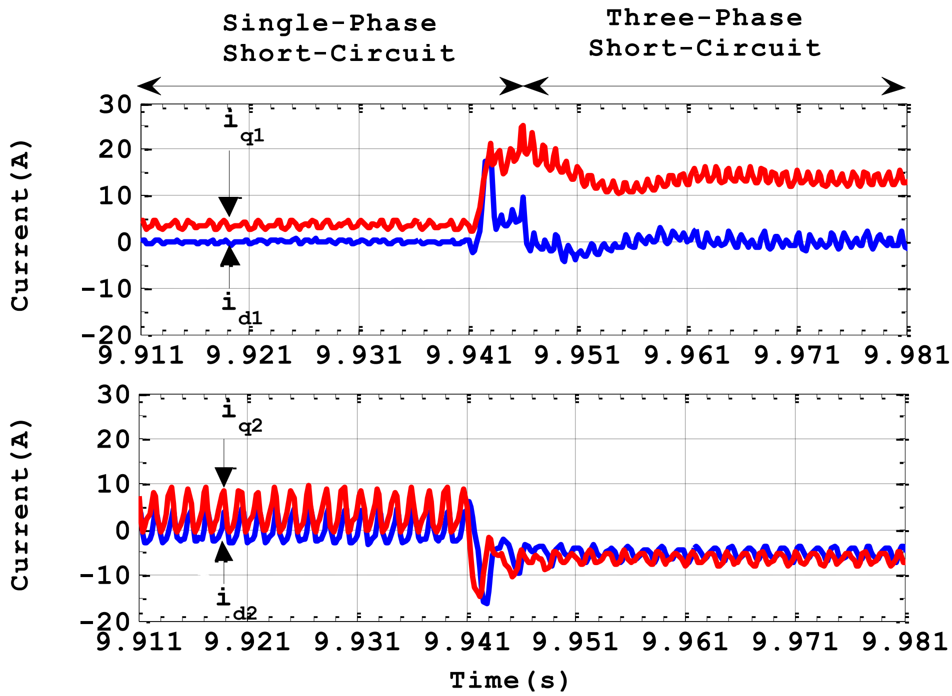

Figure 3.17 *Experimental performance of the proposed dual FS-PMSM (M_2 is short-circuited) at the speed of 2000 rad/s under single- and balanced short-operations (a) Transformed currents of motor 1. (b) Transformed currents of motor 2*

When one phase is short-circuited, the unbalanced motor impedance results in negative sequence currents and corresponding torque-ripple at twice fundamental frequency. This can be also observed in the q-axis current component of the faulty-machine in *Figure 3.17*. This is considerably reduced, as expected, when the balanced *SC* is applied. The aforementioned results clearly demonstrate the viability of this machine to operate with faults, given that the appropriate remedial control strategies are applied.

Performance during both healthy- and faulty-operations. Experimental tests have demonstrated the validity of the model. The drive has been shown to operate reliably in the presence of open-circuit and short-circuit faults with minimum braking -torque and torque-ripple. The aim of this thesis has been primarily to show the robustness of the machine and drive topology to operate under-faults originating either from the converter or from the machine itself. Further work is however required to determine the losses and, consequently, the efficiency of machine operation during both healthy- and faulty-conditions. The faulty-conditions would likely be the machine-drive sizing case if full rated operation is required after experiencing a fault. The machine-drive design optimization is an important aspect if such a system was to be adopted as many tradeoffs between machine size and efficiency, filtering requirements, and converter *VA* requirements need investigation [22].

5. FIELD-WEAKENING OPERATION

The field-oriented control is also called an indirect-control (the torque is indirectly controlled through the currents). *Figure 5.1* shows the simulation schematic of a vector-control of FS-PMSM with lookup table under no-load and with field-weakening based on voltage controller (*I-controller*). The voltage controller is using the voltage error signals between the maximum voltage output (*voltage demand*) and back-EMF (*Actual voltage*). The Back-EMF is calculated from the direct and quadrature voltages v_d and v_q. The field-weakening controller must identify all delays between the demand and actual voltage. The output of the voltage regulator (*I-regulator*) determined the required mount of the demagnetizing current (current demand). In addition, the onset of flux-weakening could be adjusted to prevent the saturation of the current regulators required by vector-controllers of FS-PMSM. Conventionally, two current controllers are always required to achieve torque (*q-axis current*) and flux (*d-axis current*) control. The reference value of quadrature current i_{sq}^{r} is obtained from the saturation limiter. The input of the saturation limiter is the reference speed and the maximum upper/lower limit of the quadrature current ($\pm i_{sq\ max}^{r}$). The maximum upper/lower limit value of the quadrature current ($\pm i_{sq\ max}^{r}$) is obtained from equation (5.1).

$$i_s^r = \sqrt{i_{sd}^{r\ 2} + i_{sq}^{r\ 2}} \le i_{s\_\max} \tag{5.1}$$

where i_{s_max} is the maximum output current.

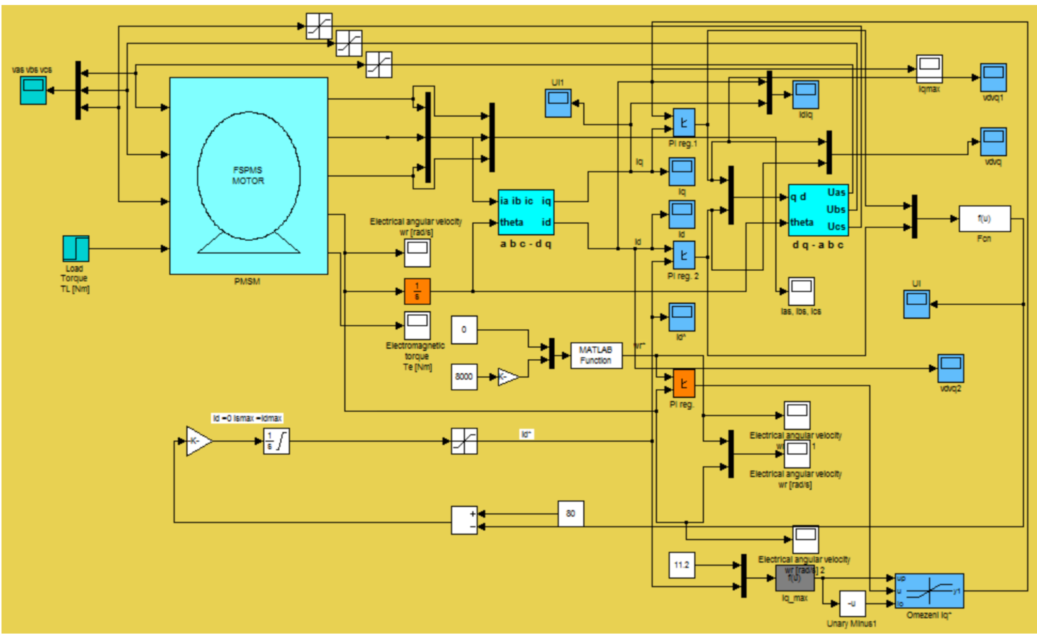

Figure 5.1 The simulation schematic of a vector-control of FS-PMSM with field-weakening based on a voltage-controller

Figure 5.2 shows the Performance of the proposed Dual FS-PMSM during operation, below and above the rated speed *7600 rpm*. The effect of field-weakening can be achieved by advancing the current vector beyond $\delta = \pi/2$ i.e. introducing a current component in the negative d-axis to create a d-axis flux in opposition to that of the stator permanent magnets, resulting in a decrease air-gap flux. As a consequence i_{sq}^{r} and then the torque are reduced in order not to exceed the maximum output current *11.2 A.*

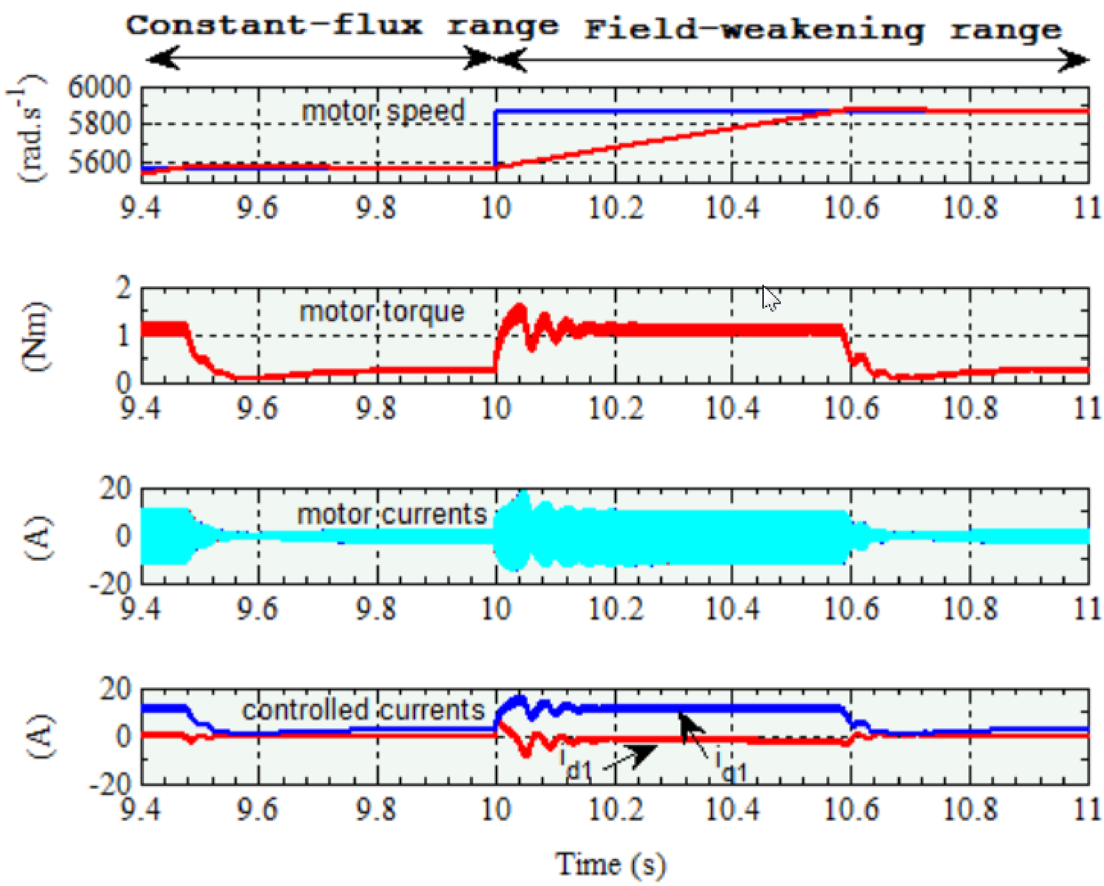

Figure 5.2 *Performance of the proposed dual FS-PMSM during operation below /above rated speed of 7600 rpm a) Motor speed (b) Motor torque (c) Motor currents (d) Transformed currents of motor 1*

Figure 5.3 shows the motor speed Performance of the proposed dual FS-PMSM during the operation (below and above the rated speed 7600 rpm). *Figure 5.4* shows the zoomed in reference voltages and motor currents under both constant-flux and field-weakening range.

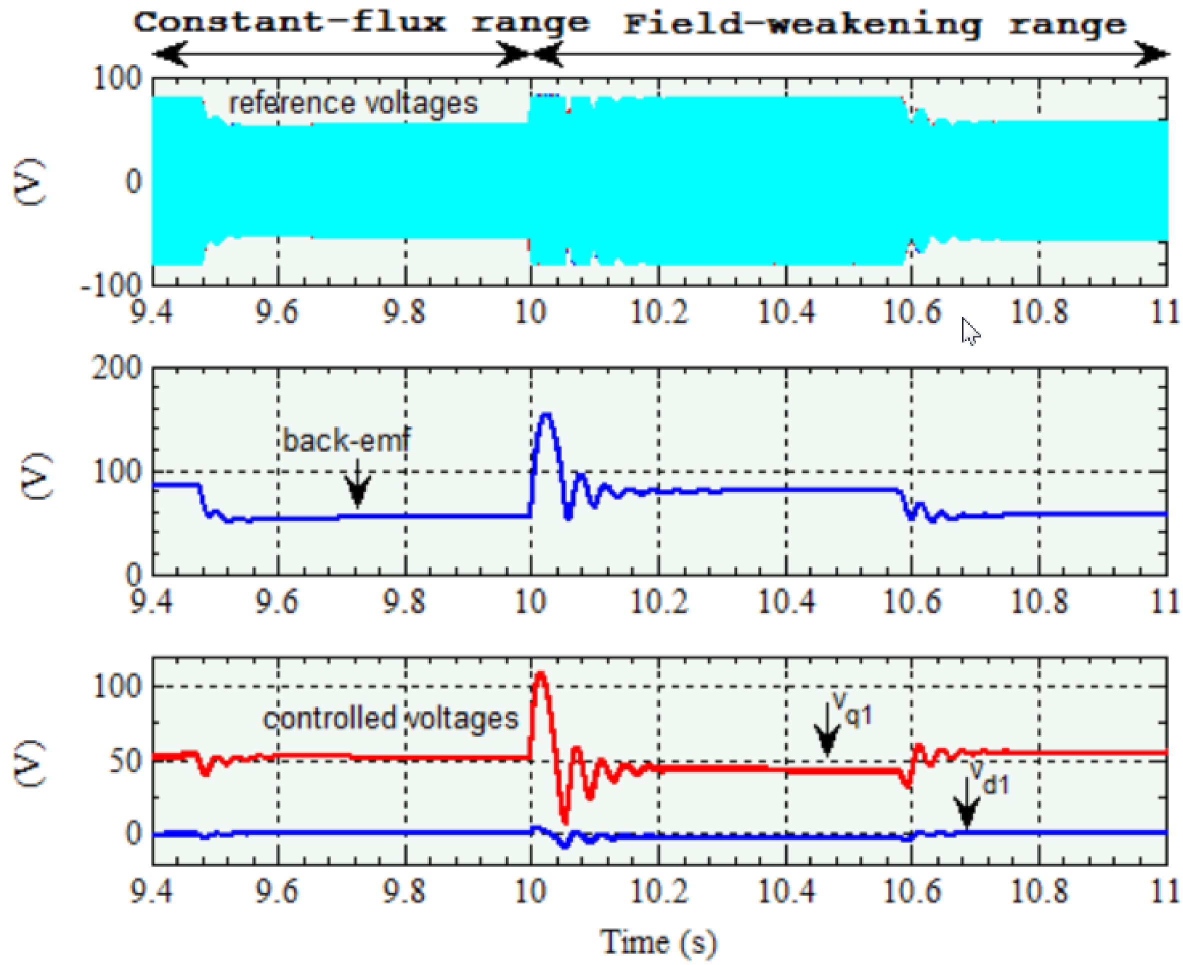

Figure 5.3 *Performance of the proposed dual FS-PMSM with during operation below/above rated speed 7600 rpm a) Reference voltages (b) Back-EMF (c) Transformed voltages of motor 1*

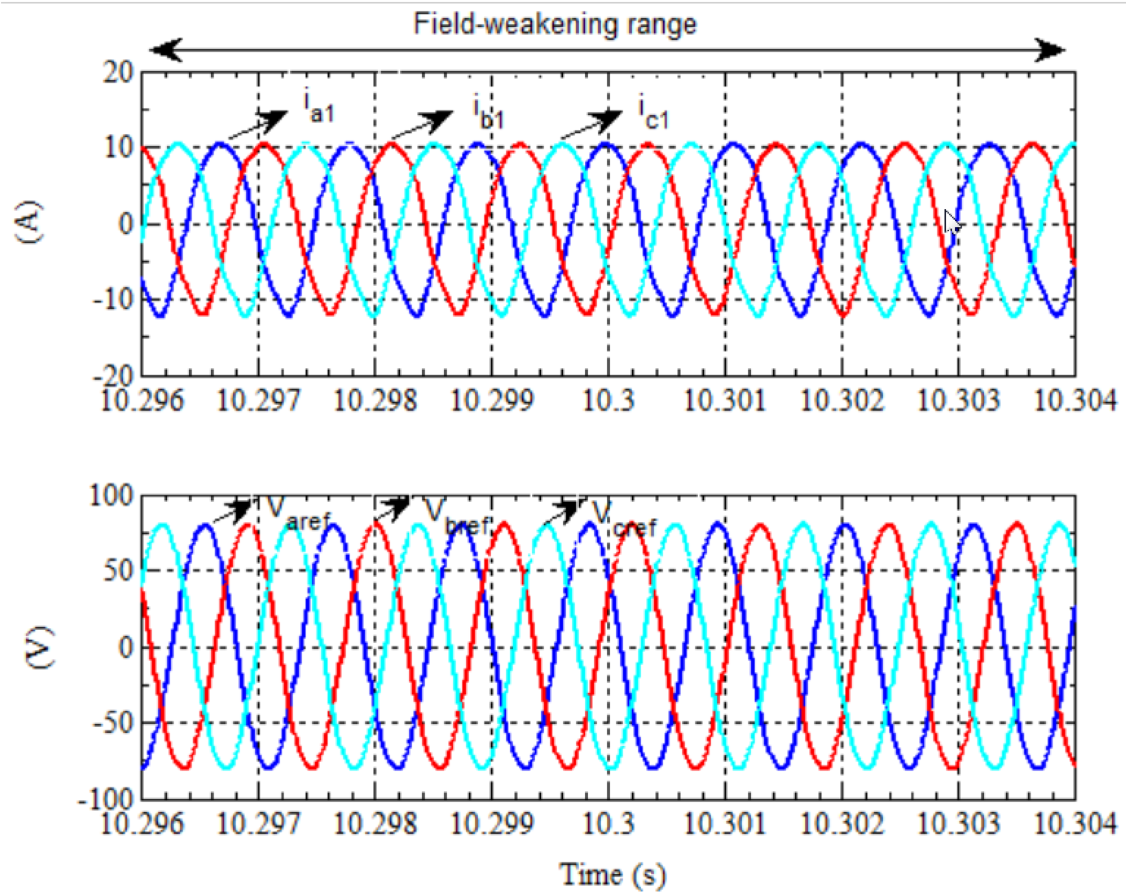

Figure 5.4 *Performance of the proposed dual FS-PMSM with during operation below/above rated speed 7600 rpm a) Reference voltages (b) Motor currents (Zoomed in) (c) Transformed voltages of motor 1 (zoomed in)*

6. CONCLUSION

Electrical servodrive is a control drive, consisting of one or more electrical motors, which is fed by an electronic power-converter which is powered by semiconductor devices and controlled by electronic circuits. The electronic power-converter converts voltage and current from one to another applying power electronics device in the power circuit and microelectronics circuits to control the input-output values of the converter.

This thesis presents a fault-tolerant flux-switching permanent magnet motor drive control system driven by a six-phase voltage source inverter. A dual three-phase flux-switching permanent magnet motor, which consists of two separate three-phase stator windings, has an ability to provide the fault-tolerant capability under faulty-operating conditions. In the event of faults when the one three-phase motor stops working, the remaining healthy three-phase motor can continue to operate unaffected. In addition, this modular approach also provides the minimal electrical, magnetic and thermal interaction between phases of the drive. The dual three-phase flux-switching permanent magnet motor model is created in order to investigate the behaviour of the motor drive control system under healthy- and faulty-operating conditions. Moreover, the field-orientated indirect vector-control is employed to control the drive system at a wide range of speeds and load-torque applied. Under the fault-operation mode the modified control strategy is adopted to the drive system in order to keep the motor operating continuously as well as to maintain the system performance as before the fault occurrence. The simulations of the considered motor drive control system have been carried out using *Matlab-Simulink.* The simulation results of the entire system operating with no-load and load-torque applied are presented under both normal- and fault-operating conditions. The experimental setup is implemented to validate the effectiveness of the fault-tolerant flux-switching motor drive control system operating under a wide range of operations even in the presence of a fault. The simulation and the experimental results show that the proposed fault-tolerant flux-switching permanent magnet motor drive system has an ability to maintain the system performance under both normal- and fault-operation modes.

This thesis has demonstrated the operability of a flux-switching machine as an integral part of a high-performance fault-tolerant vector-controlled drive. A nonlinear-machine model has been described, which is able to predict the drive's performance during both healthy- and faulty-operations. Experimental tests have demonstrated the validity of the model. The drive has been shown to operate reliably in the presence of open-circuit and short-circuit faults with minimum braking-torque and torque-ripple.

The aim of this thesis has been has been primarily to show the robustness of the machine and drive topology to operate under-faults originating either from the converter or from the machine itself. Further work is however required to determine the losses and, consequently, the efficiency of machine operation during both healthy- and faulty-conditions. The faulty-conditions would likely be the machine-drive sizing case if full rated operation is required after experiencing a fault. The machine-drive design optimization is an important aspect if such a system was to be adopted as many tradeoffs between machine size and efficiency, filtering requirement, and converter VA requirement need investigation. Both simulated and experimental results verify that the FS-PMSM can be operated effectively by adopting the developed control strategy and offers good steady-state and dynamic performance.

7. BIBLIOGRAPHY

[1] Y. Pang, Z. Q. Zhu, D. Howe, S. Iwasaki, R. Deodhar, and A. Pride,“Comparative study of flux-switching and interior permanent-magnet machines,” in *Proc. ICEMS*, Oct. 2007, pp. 757–762.

[2] W. Zhao, M. Cheng, W. Hua, and H. Jia, “A redundant flux-switching permanent-magnet motor drive for fault-tolerant applications,” in Proc. IEEE VPPC, Sep. 2008, pp. 1–6.

[3] B. C. Mecrow, A. G. Jack, J. A. Haylock, and J. Coles, “Fault-tolerant permanent-magnet machine drives,” Proc. Inst. Elect. Eng.—Elect. Power Appl., vol. 143, no. 6, pp. 437–442, Nov. 1996.

[4] K. T. Chau, C. C. Chan, and C. Liu, “Overview of permanent-magnet brushless drives for electric and hybrid electric vehicles,” IEEE Trans. Ind. Electron., vol. 55, no. 6, pp. 2246–2257, Jun. 2008.

[5] A. M. El-Refaie, “Fault-tolerant permanent magnet machines,” IET Elect. Power Appl., vol. 5, no. 1, pp. 59–74, Jan. 2011.

[6] D. Gerada, A. Mebarki, and C. Gerada, “Optimal design of a high speed concentrated wound PMSM,” in Proc. ICEMS, Nov. 2009, pp. 1–6.

[7] T. Raminosoa, C. Gerada, N. Othman, and L. D. Lillo, “Rotor losses in fault-tolerant permanent-magnet synchronous machines,” IET Elect. Power Appl., vol. 5, no. 1, pp. 75–88, Jan. 2011.

[8] J. W. Bennett, G. J. Atkinson, B. C. Mecrow, and D. J. Atkinson, “Fault-tolerant design considerations and control strategies for aerospace drives,” IEEE Trans. Ind. Electron., vol. 59, no. 5, pp. 2049–2058, May 2012.

[9] S. J. Nall and P. H. Mellor, “A compact direct-drive permanent-magnet motor for a UAV rotorcraft with improved faulted behaviour through operation as four separate three-phase machines,” in Proc. IET Int. Conf. PEMD, Apr. 2008, pp. 245–249.

[10] L. Alberti and N. Bianchi, “Impact of winding arrangement in dual threephase induction motor for fault-tolerant applications,” in Proc. ICEMS, Sep. 2010, pp. 1–6.

[11] T. Raminosoa and C. Gerada, “Novel fault-tolerant design of flux-switching machines,” in Proc. IET Int. Conf. PEMD, Apr. 2010, pp. 1–6.

[12] T. Raminosoa, C. Gerada, and M. Galea, “Design considerations for a fault-tolerant flux-switching permanent-magnet machine,” IEEE Trans. Ind. Electron., vol. 58, no. 7, pp. 2818–2825, Jul. 2011.

[13] T. Raminosoa and C. Gerada, “Fault-tolerant winding technology comparison for flux-switching machine,” in Proc. ICEM, Sep. 2010, pp. 1–6.

[14] W. Zhao, M. Cheng, K. T. Chau, J. Ji, W. Hua, and R. Cao, “A new modular flux-switching permanent-magnet machine using fault-tolerant teeth,” in Proc. IEEE CEFC, May 2010, p. 1.

[15] J. T. Chen and Z. Q. Zhu, “Comparison of all and alternate poles wound flux-switching PM machines having different stator and rotor pole numbers,” IEEE Trans. Ind. Electron., vol. 46, no. 4, pp. 1406–1415, Aug. 2010.

[16] M. Cheng, W. Hua, J. Zhang, and W. Zhao, “Overview of statorpermanent-magnet brushless machines,” IEEE Trans. Ind. Electron., vol. 58, no. 11, pp. 5087–5101, Nov. 2011.

[17] J. T. Chen and Z. Q. Zhu, “Influence of rotor pole number on optimal parameters in flux-switching PM brushless ac machines by lumped parameter magnetic circuit model,” in Proc. IEEE IEMDC, May 2009, pp. 1216–1223.

[18] W. Zhao, M. Cheng, W. Hua, H. Jia, and R. Cao, “Back-EMF harmonic analysis and fault-tolerant control of flux-switching permanent-magnet machine with redundancy,” IEEE Trans. Ind. Electron., vol. 58, no. 5, pp. 1926–1935, May 2011.

[19] W. Zhao, M. Cheng, K. T. Chau, W. Hua, H. Jia, J. Ji, and W. Li, “Stator-flux-oriented fault-tolerant control of flux-switching permanentmagnet motors,” IEEE Trans. Magn., vol. 47, no. 10, pp. 4191–4194, Oct. 2011.

[20] J. J. Wolmarans, H. Polinder, J. A. Ferreira, and D. Clarenbach, “Selecting an optimum number of system phases for an integrated, faulttolerant permanent-magnet machine and drive,” in Proc. EPE, Sep. 2009, pp. 1–10.

[21] Y. Zhang, J. Zhu,W. Xu, and Y. Guo, “A simple method to reduce torqueripple in direct torque-controlled permanent-magnet synchronous motor by using vectors with variable amplitude and angle,” IEEE Trans. Ind. Electron., vol. 58, no. 7, pp. 2848–2859, Jul. 2011.

[22] M. O. E. Aboelhassan. T. Raminosoa, A. goodman, L. de Lillo, C. Gerada, “Performance evaluation of a vector-control fault-tolerant flux-switching motor drive,” IEEE Trans. Ind. Electron., vol. 60, no. 8, pp. 2997-3006, August 2013.

ABSTRACT

It has become clear that the most successful design approach involves a multiple phase drive in which each phase may be regarded as a single-module. The operation of any one module must have minimal impact upon the others, so that in the event of that module failing the others can continue to operate unaffected. The modular approach requires that there should be minimal electrical, magnetic and thermal interaction between phases of the drive. Flux-Switching permanent magnet synchronous machines (FS-PMSM) have recently emerged as an attractive machine type virtue of their high torque densities, simple and robust rotor structure and the fact that permanent magnets and coils are both located on the stator.

Flux-switching permanent magnet (FS-PMSM) synchronous machines are a relatively new topology of stator PM brushless machine. They exhibit attractive merits including the large torque capability and high torque (power) density, essentially sinusoidal back-EMF waveforms, as well as having a compact and robust structure due to both the location of magnets and armature windings in the stator instead of the rotor as those in the conventional rotor-PM machines. The comparative results between a FS-PMSM and a traditional surface-mounted PM (SPM) motor having the same specifications reveal that FS-PMSM exhibits larger air-gap flux density, higher torque per copper loss, but also a higher torque-ripple due to cogging-torque. However, for solely permanent magnets excited machines, it is a traditional contradiction between the requests of high torque capability under the base-speed (constant torque region) and wide speed operation above the base speed (constant power region) especially for hybrid vehicle applications.

A novel fault-tolerant FS-PMSM drive topology is presented, which is able to operate during open- and short-circuit winding and converter faults. The scheme is based on a dual winding motor supplied from two separate vector-controlled voltage-sourced inverter drives. The windings are arranged in a way so as to form two independent and isolated sets. Simulation and experimental work will detail the driver’s performance during both healthy- and faulty-scenarios including short-circuit faults and will show the drive robustness to operate in these conditions.

The work has been published in ten conference papers, two journal papers and a book chapter, presenting both the topology of the drive and the applied control schemes, as well as analysing the fault-tolerant capabilities of the drive.

ABSTRAKT

Je jasné, že nejúspěšnější konstrukce zahrnuje postup vícefázového řízení, ve kterém každá fáze může být považována za samostatný modul. Provoz kterékoliv z jednotek musí mít minimální vliv na ostatní, a to tak, že v případě selhání jedné jednotky ostatní mohou být v provozu neovlivněny. Modulární řešení vyžaduje minimální elektrické, magnetické a tepelné ovlivnění mezi fázemi řízení (*měniče*). Synchronní stroje s pulzním tokem a permanentními magnety se jeví jako atraktivní typ stroje, jejíž přednostmi jsou vysoký kroutící moment, jednoduchá a robustní konstrukce rotoru a skutečnost, že permanentní magnety i cívky jsou umístěny společně na statoru.

FS-PMSM jsou poměrně nové typy střídavého stroje stator-permanentní magnet, které představují významné přednosti na rozdíl od konvenčních rotorů - velký kroutící moment, vysoký točivý moment, v podstatě sinusové zpětné EMF křivky, zároveň kompaktní a robustní konstrukce díky umístění magnetů a vinutí kotvy na statoru. Srovnání výsledků mezi FS-PMSM a klasickými motory na povrchu upevněnými PM (SPM) se stejnými parametry ukazuje, že FS-PMSM vykazuje větší vzduchové mezery hustoty toku, vyšší točivý moment na ztráty v mědi, ale také vyšší pulzaci díky reluktančnímu momentu. Pro stroje buzené permanentními magnety se jedná o tradiční rozpor mezi požadavkem na vysoký kroutící moment pod základní rychlostí (*oblast konstantního momentu*) a provozem nad základní rychlostí (*oblast konstantního výkonu*), zejména pro aplikace v hybridních vozidlech.

Je předložena nová topologie synchronního stroje s permanentními magnety a spínaným tokem odolného proti poruchám, která je schopná provozu během vinutí naprázdno a zkratovaného vinutí i poruchách měniče. Schéma je založeno na dvojitě vinutém motoru napájeném ze dvou oddělených vektorově řízených napěťových zdrojů. Vinutí jsou uspořádána takovým způsobem, aby tvořila dvě nezávislé a oddělené sady. Simulace a experimentální výzkum zpřesní výkon během obou scénářů jak za normálního provozu, tak za poruch včetně zkratových závad a ukáží robustnost pohonu za těchto podmínek.

Tato práce byla publikována v deseti konferenčních příspěvcích, dvou časopisech a knižní kapitole, kde byly představeny jak topologie pohonu a aplikovaná řídící schémata, tak analýzy jeho schopnosti odolávat poruchám.